MICROSTRUCTURES AND ORIGINS OF TWO CORUNDUM-HIBONITE INCLUSIONS FROM ALH A77307 (CO3.0). Jangmi Han[1,2], Lindsay P. Keller[2], Andrew W. Needham[2,3], Scott Messenger[2], and Justin I. Simon[2]. [1]Lunar and Planetary Institute, Houston, TX 77058, USA (jangmi.han@nasa.gov), [2]ARES, NASA/JSC, Houston, TX 77058, USA, [3]Oak Ridge Associated Universities, Oak Ridge, TN 37830, USA.

Introduction: Equilibrium condensation calculations for a gas of solar composition predict corundum as one of the earliest-formed refractory phases [1]. On cooling, corundum is believed to react with a nebular gas to form hibonite [1]. Corundum-bearing CAIs are relatively rare [2]. While some show textural and compositional evidence for a direct condensation origin [3], corundum can also form by partial evaporation of hibonite [4]. Therefore, a detailed investigation of textural relationship between corundum and hibonite is required to understand their origins and also provide important insights into conditions and processes in the early, high-temperature stages of the solar system.

Previous O and Mg isotopic studies of two corundum-hibonite inclusions from ALH A77307 (CO3.0) suggest that they experienced different formation histories [5,6]. We used TEM to investigate the fine scale mineralogy and petrography of these CAIs from ALH A77307 in order to provide the context for the isotopic data and additional constraints on their formation conditions and processes.

Methods: We prepared three FIB sections from two corundum-hibonite CAIs (61 and 160) in ALH A77307 using a FEI Quanta 600 3D dual beam FIB-SEM, after NanoSIMS analyses [5,6]. The FIB sections were characterized in detail using a JEOL 2500SE field-emission scanning TEM. In addition, chemical microanalyses and mapping were carried out using a Thermo-Noran thin-window energy dispersive x-ray spectrometer.

Results: CAI-61 is compact and irregular in shape with a size of 24×25 μm. This CAI consists of a hibonite core partially surrounded by corundum and spinel; the hibonite core is in partial contact with the surrounding matrix. A partial rim of high-Ca pyroxene 0.5-1 μm in thickness occurs on one side of the CAI. Surrounding the hibonite core are partial layers of corundum (0.5-3 μm in thickness), often followed by spinel layers (0.3-1 μm in thickness). Two of the spinel grains are in direct contact with the hibonite core.

CAI-160 is irregularly-shaped, porous object 14×15 μm in size. The CAI consists of aggregates of corundum grains with minor hibonite grains. Three hibonite grains are present and have somewhat different textural occurrences: (1) a rounded grain 1 μm in diameter surrounded by corundum on one side of the CAI, (2) an elongated hibonite grain 5 μm long enclosed by corundum in the center of the CAI, and (3) a 2×3 μm sized grain in partial contact with corundum on the other side of the CAI.

Two FIB sections from CAI-61 (61-A and -B) were prepared as transects from one edge through the hibonite core to the other edge. Both sections consist of a core of hibonite grains (1.5-13 μm in size) surrounded by an intergrowth of corundum and spinel. Surrounding the hibonite core in both FIB sections is an intergrowth layer of corundum and spinel. In these layers, corundum grains are in direct contact with the hibonite core and often have embayed grain boundaries toward the hibonite core. Spinel grains in the layers occur either on the hibonite core or on the corundum grains. In FIB 61-A, the intergrowth layers 0.3-0.7 μm in thickness consisting of elongated corundum (0.1-0.7 μm thick and 0.7-3.5 μm long) and spinel (0.2-0.7 μm thick and 0.4-1.2 μm long) grains occur on both sides of the hibonite core. FIB 61-B contains a layer 0.3-2.5 μm in thickness of corundum and spinel surrounding one side of the hibonite core. The corundum grains (0.4-3.5 μm in size) are elongated to subrounded, but the spinel grains are irregular in shape and range in size from 0.2 to 2.5 μm. In addition, both FIB sections contain relatively larger corundum grain(s) adjacent to the hibonite core: two 2-5 μm sized grains at the bottom of the core in FIB 61-A and one 7 μm sized grain at the side of the core in FIB 61-B. Finally, a 0.3-0.6 μm thick rim of high-Ca pyroxene with grain sizes of 0.3-1 μm is present in FIB 61-B. Elemental X-ray maps of the pyroxene rim reveal a gradual decrease of Al concentration and a gradual increase of Mg and Si concentration outward from the interface with spinel.

TEM observations from CAI-61 show that there is an epitaxial relationship between hibonite and spinel (Fig. 1). Analysis of electron diffraction patterns and the Fast Fourier Transform (FFT) patterns obtained from HR-TEM images of hibonite and spinel grains from both FIB sections yields the same crystallographic orientation relationships between them: $(001)_{hibonite}$ // $(111)_{spinel}$.

One FIB section from CAI-160 (160-A) was prepared across the three hibonite grains. The FIB section is dominated by corundum with three hibonite grains. The hibonite grains 1-2.5 μm in size have curved grain boundaries. A subrounded refractory metal nugget 50 nm in diameter occurs as an inclusion in corundum.

Three FIB sections from CAIs-61 and -160 share several TEM observations. (1) Corundum is free of defects and is nearly pure Al_2O_3 with uniform compositions within and between grains as well as between FIB

sections. (2) Hibonite is very close to $CaAl_{12}O_{19}$ with only minor Ti and no detectable Mg and Si. The Ti X-ray maps reveals that Ti concentrations are constant in the core of hibonite grains, but shows an increase within 10-30 nm of grain boundaries with corundum and spinel. (3) No crystallographic orientation relationships of corundum with hibonite or spinel have been observed (Fig. 1).

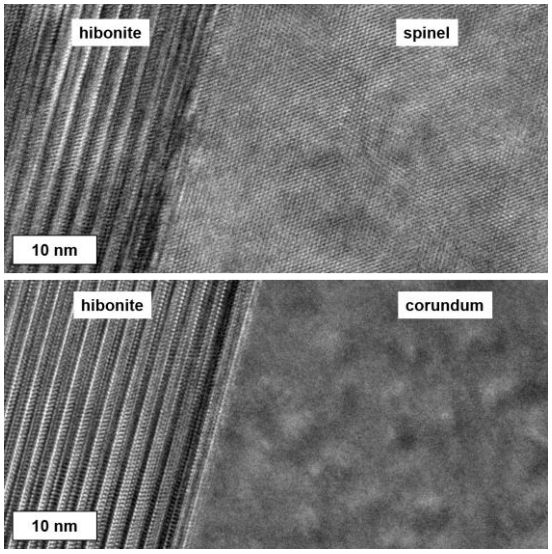

Figure 1. HR-TEM images of the interfaces of hibonite-spinel (upper) and hibonite-corundum (bottom), showing the crystallographic continuity only between hibonite and spinel.

Discussion: The observed textural relationships between corundum and hibonite from two corundum-hibonite CAIs indicate that hibonite is the first phase to form, followed by corundum. Also, our TEM observations from CAI-61 indicate the direct overgrowth of spinel on hibonite and corundum without melilite or perovskite. This inferred formation sequence is inconsistent with the predicted equilibrium condensation sequence from a gas of solar composition at total pressure $<10^{-2}$ bar [1].

We explore two possible scenarios for the formation of corundum after hibonite: (1) partial melting and evaporation of hibonite and (2) condensation under variable physico-chemical conditions. In the first scenario, early-formed hibonite may have experienced partial melting, followed by evaporative loss of Ca and late crystallization of corundum [4,7]. The unmelted, residual hibonite would be embayed and enclosed by corundum grains, forming a compact object similar to CAI-61. However, the required melting temperature of hibonite to form an Al-rich liquid or a corundum + Ca-rich liquid is >2,100 K, which requires high dust/gas ratios [3,4]. In addition, formation of corundum on hibonite by evaporation is expected to result in mass dependent fractionation of O and Mg isotopes. No mass dependent fractionation of O and Mg isotopes was observed for corundum and hibonite in both CAIs [5,6]. Therefore the breakdown of hibonite by evaporation appears not to be an important mechanism for the formation of these CAIs.

An alternative formation mechanism is condensation of corundum after hibonite under variable physico-chemical conditions. A change in total pressure and/or dust/gas enrichment of a gas affects the sequence in which minerals condense in a cooling nebular gas [1]. For example, at total pressure $>10^{-3}$ bar, hibonite is predicted to condense before corundum from a cooling gas of solar composition [8]. One possibility is that the hibonite core is relict and was transported to a hotter region of the solar nebula where corundum condensed later [9]. Additionally, the highly irregular shape of hibonite and corundum and the lack of mass dependent fractionation of O and Mg isotopes in the two CAIs [5,6] support their condensation origin.

Following the condensation of corundum on hibonite, corundum in CAI-160 was isolated from the nebular gas, probably by a physical removal from a region of the solar nebula where major elements (Si, Mg, and Fe) were still condensing.

In CAI-61, some spinel grains that occur next to the hibonite core, surrounded by another spinel grains, are in crystallographic continuity with the hibonite core. These observations suggest that early-condensed spinel epitaxially nucleated and grew directly onto hibonite [10], followed by the later condensation of the majority of randomly-oriented spinel. The final stage to form CAI-61 was pyroxene condensation to form a partial rim.

Conclusions: Textural evidence for the late formation of corundum on hibonite in the two corundum-hibonite CAIs in ALH A77307 suggest that their formation processes cannot be easily explained by a simple equilibrium condensation. Combined isotopic data and TEM observations suggest that these corundum-hibonite CAIs may have formed by condensation under specific conditions (e.g., at higher total pressure).

Acknowledgements: This research was supported by grant 10-COS10-0049 to L.P. Keller (PI).

References: [1] Ebel D. S. (2006) MESS2 pp.253-277. [2] MacPherson G. J. (2014) Treatise on Geochemistry II vol.1 pp.139-179. [3] Simon S.B. et al. (2002) Meteoritics & Planet. Sci., 37, 533-548. [4] MacPherson G.J. et al. (1984) JGR 89, C299-C312. [5] Needham A.W. & Messenger S. (2012) 75th MAPS, Abstract #5384. [6] Needham A.W. & Messenger S. (2013) LPS XXXXIV, Abstract #2929. [7] Floss C. et al. (1998) Meteoritics & Planet. Sci., 33, 191-206. [8] Petaev M.I. and Wood J. A. (2005) Chondrites and the Protoplanetary Disk, pp.1123-1137. [9] Simon J.I. et al. (2011) Science 331, 1175-1178. [10] Han J. & Brearley A.J. (2014) LPS XLV, Abstract #2125.